Am J Physiol Regul Integr Comp Physiol 313: R78–R90, 2017.
First published May 12, 2017; doi:10.1152/ajpregu.00351.2016.

RESEARCH ARTICLE | *Fluid and Electrolyte Homeostasis*

Flexible ammonia handling strategies using both cutaneous and branchial epithelia in the highly ammonia-tolerant Pacific hagfish

Alexander M. Clifford,[1,2] Alyssa M. Weinrauch,[1,2] Susan L. Edwards,[2,3] Michael P. Wilkie,[2,4] and Greg G. Goss[1,2]

[1]*Department of Biological Sciences, University of Alberta, Edmonton, Alberta, Canada;* [2]*Bamfield Marine Sciences Centre, Bamfield, British Columbia, Canada;* [3]*Department of Biology, Appalachian State University, Boone, North Carolina; and* [4]*Department of Biology and Laurier Institute for Water Science, Wilfrid Laurier University, Waterloo, Ontario, Canada*

Submitted 15 August 2016; accepted in final form 8 May 2017

Clifford AM, Weinrauch AM, Edwards SL, Wilkie MP, Goss GG. Flexible ammonia handling strategies using both cutaneous and branchial epithelia in the highly ammonia-tolerant Pacific hagfish. *Am J Physiol Regul Integr Comp Physiol* 313: R78–R90, 2017. First published May 12, 2017; doi:10.1152/ajpregu.00351.2016.—Hagfish consume carrion, potentially exposing them to hypoxia, hypercapnia, and high environmental ammonia (HEA). We investigated branchial and cutaneous ammonia handling strategies by which Pacific hagfish (*Eptatretus stoutii*) tolerate and recover from high ammonia loading. Hagfish were exposed to HEA (20 mmol/l) for 48 h to elevate plasma total ammonia (T_{Amm}) levels before placement into divided chambers for a 4-h recovery period in ammonia-free seawater where ammonia excretion (J_{Amm}) was measured independently in the anterior and posterior compartments. Localized HEA exposures were also conducted by subjecting hagfish to HEA in either the anterior or posterior compartments. During recovery, HEA-exposed animals increased J_{Amm} in both compartments, with the posterior compartment comprising ~20% of the total J_{Amm} compared with ~11% in non-HEA-exposed fish. Plasma T_{Amm} increased substantially when whole hagfish and the posterior regions were exposed to HEA. Alternatively, plasma T_{Amm} did not elevate after anterior localized HEA exposure. J_{Amm} was concentration dependent (0.05–5 mmol/l) across excised skin patches at up to eightfold greater rates than in skin sections that were excised from HEA-exposed hagfish. Skin excised from more posterior regions displayed greater J_{Amm} than those from more anterior regions. Immunohistochemistry with hagfish-specific anti-rhesus glycoprotein type c (α-hRhcg; ammonia transporter) antibody was characterized by staining on the basal aspect of hagfish epidermis while Western blotting demonstrated greater expression of Rhcg in more posterior skin sections. We conclude that cutaneous Rhcg proteins are involved in cutaneous ammonia excretion by Pacific hagfish and that this mechanism could be particularly important during feeding.

cyclostome; nitrogen; rhesus glycoprotein; skin; agnatha

HAGFISHES are distributed throughout the world's oceans, and along with the lampreys, are one of two families of extant jawless fishes that diverged from the vertebrate lineage ~500 million years ago (2). Hagfishes are also well-known scavengers, feeding on carrion that falls to the ocean bottom (35). Feeding opportunities may include marine mammals (44) and more commonly, fishes, including commercial by-catch (17). Adaptations for this feeding lifestyle include a protrusible dental plate capable of tearing flesh and burrowing into carrion (11), high tolerance to hypoxic and anoxic conditions (18), and the ability to acquire amino acids (26) and phosphate (42) across the skin and gill epithelia, in addition to the intestine (for review see Ref. 13). The high tolerance to ammonia observed in hagfishes may be related to their scavenging lifestyle by which they may routinely encounter extremely high concentrations of ammonia while burrowing into the decomposing carcasses of fishes and large marine mammals (13, 14, 46, 54). Currently there are no data characterizing the biochemical processes of putrefaction during marine-based decomposition. However, in terrestrial environments, mammalian decomposition produces high amounts of putrefactive compounds including hydrogen sulfide, methane, amino acids, and pertinent to the current study, $(NH_4)_2SO_4$, which is deposited in the surrounding soil at levels exceeding 525 μg/g (~29 mmol/l; see Ref. 7). As many of the microflora involved in the putrefactive process arise from the gut (7), it is reasonable to infer that decomposing aquatic organisms also produce high amounts of ammonia and immersion of the branchial region of hagfishes into the carcass would subject this region to high amounts of ammonia, which would result in the accumulation of ammonia in the hagfish. In contrast, the posterior region of the animal is usually left exposed to seawater where the concentration of ammonia would be lower and likely favor excretion, provided that the appropriate transport mechanisms and gradients are present.

In most teleost fishes, ammonia toxicity arises when plasma ammonia concentrations exceed 1 mmol/l, leading to gill damage, metabolic disturbances, and disruption of the central nervous system as characterized by pronounced swelling of the brain (55), hyperexcitability, coma, and eventually death (see Refs. 29, 43, 50 for reviews). A number of tropical fishes however, including the weatherloach (*Misgurnus anguilla caudatus;* 9, 48), mudskipper (*Periophthalmodon schlosseri*; 30), and snakehead (*Channa asiatica*; 10) can withstand exposure to ammonia concentrations ranging up to 100 mmol/l. The ammonia-tolerant Pacific hagfish (*Eptatretus stoutii*) readily survives 48 h exposure to 20 mmol/l total ammonia (T_{Amm}), which results in plasma ammonia concentrations of 5.7 mmol/l, the highest amount reported in any chordate (14). Furthermore, hagfish are also apparently capable of excreting ammonia against large, inwardly directed gradients during high environmental ammonia (HEA) exposure through active excretion

Address for reprint requests and other correspondence: A. M. Clifford, Dept. of Biological Sciences, University of Alberta, 116 St. and 85 Ave., Edmonton, Alberta T6G 2R3, Canada (e-mail: alex.clifford@ualberta.ca).

(14). While the mechanism(s) responsible for this capability remains elusive, the potential exists that the gills and/or skin of the hagfish can be relatively impermeable to ammonia, which may aid in their ammonia handling abilities.

The overarching goal of the present study was to investigate the relative roles of the gill and skin of Pacific hagfish in ammonia uptake and excretion during and after exposure to HEA. We hypothesized that there are differential nitrogen-handling strategies employed between the anterior and posterior segments of the Pacific hagfish as a result of their immersing themselves into carrion as they feed, which may incidentally lead to ammonia uptake in the anterior (branchial) region, but excretion via posterior routes.

In the teleost gill, Rhesus glycoprotein type c (Rhcg) acts as a facilitated ammonia transporter (SLC 42 transporter family; Ref. 57) and has been recently localized to the gill and skin of Atlantic hagfish (*Myxine glutinosa*) and termed hRhcg (22). Similarly, the Pacific hagfish gill has previously been shown to express Rhbg and Rhcg1 using immunohistochemistry (IHC; Ref.4). The presence of Rhcg in both the gill and skin of hagfishes suggests that it likely plays an important role in modulating J_{Amm} by both routes.

In the present study, the sites of ammonia flux (J_{Amm}) before, during, and following exposure to HEA (20 mmol/l) were measured in Pacific hagfish using divided chambers to establish the relative role of anterior (branchial) versus posterior (skin) routes of ammonia uptake and excretion. Isolated skin patches were also used to measure ammonia flux and Western blot, and IHC was employed to investigate the mechanisms of ammonia transport in the anterior and posterior regions of the hagfish. We were particularly interested in determining whether Rhcg was differentially expressed along the length of the skin of Pacific hagfish thereby providing a mechanistic understanding of how J_{Amm} is facilitated in these ancient, highly ammonia-tolerant fishes.

MATERIALS AND METHODS

Experimental Animals and Holding

Pacific hagfish (*E. stoutii; N* = 78; average mass = 139.03 g; range = 95.85–199.45 g) were captured from Trevor channel near Bamfield, BC, Canada and held at Bamfield Marine Sciences Centre (BMSC) as previously described (15). Hagfish were fasted for 1 wk before experimentation to minimize the effects of postprandial nitrogenous waste production and excretion and defecation on experiments. All animals were used under licenses of the Department of Fisheries and Oceans Canada (permit no. XR-223 2013; XR-192 2014) and approved animal care protocol from BMSC (RS-13-24) and University of Alberta (00001126).

Chemicals

All chemicals, reagents, and enzymes were purchased from Sigma-Aldrich Chemical (St. Louis, MO), unless otherwise noted.

Experimental Protocols

Series 1: sites of ammonia excretion following exposure HEA. Hagfish were transferred to 10.0-liter, darkened buckets receiving continuously flowing seawater and left overnight to acclimate to the experimental setup. The following morning, hagfish were removed and anesthetized [0.5 g/l tricaine methanesulfonate (TMS); Syndel, Nanaimo, British Columbia, Canada; neutralized with 0.15 g/l NaOH] and a preexposure blood sample (200 μl) was drawn from the subcutaneous sinus using a heparinized 21-gauge needle for blood and plasma acid/base/ammonia analysis. Immediately after the blood sampling of lightly anesthetized hagfish, the animals were exposed to HEA (nominal $[NH_4Cl]$ = 20 mmol/l; pH 7.5) in 5.0-liter aerated seawater for 48 h. Simultaneous control (no HEA) animals were sampled and held in the same manner. After 48 h, both the control and HEA-exposed hagfish were anesthetized and weighed, and blood was collected as described above with the puncture wound sealed using cyanoacrylate glue and a small square (~4 mm^2) of nitrile rubber. Immediately after the blood sample collection while hagfish were still lightly anesthetized, animals were fitted into separating collar assemblies, briefly rinsed in anesthesia-free seawater (~30 s) to clear anesthetic, and then placed into divided chambers that isolated the posterior body region from the anterior region containing the gill pores (see Ref. 15 for apparatus and protocol details). Nominally ammonia-free seawater containing no anesthetic was then added to the anterior compartment only, and seal efficacy was checked by monitoring water appearance in the posterior compartment. Ammonia-free seawater was then added to the posterior compartment and a lid secured. The chamber was placed in a wet table receiving flowing seawater for temperature control (~10°C). Water samples (1 ml) for ammonia quantification were collected and acidified to ~pH 4.1 with 1 μl of 1 N HCl to prevent NH_3 volatilization and immediately frozen following both the placement of hagfish into the chamber and following the recovery period. After final sample collection, the patency of the seal was visually inspected, the hagfish were removed from the apparatus and killed by TMS overdose (5 g/l TMS neutralized with 1.5 g/l NaOH), and a final blood sample was collected (as stated above).

To evaluate the potential contribution of the cloaca to ammonia excretion, the cloaca was sealed in a subset of experimental animals (n = 8) with a rubber bandage and cyanoacrylate glue. No differences were detected in ammonia efflux in the posterior compartment in animals with or without this seal.

To rule out artifacts, the divided chamber apparatus was tested for leaks by measuring Mg^{2+} flux as a proxy for leakage. Hagfish (n = 6) were fitted into the chambers (as describd above), and artificial seawater (ASW; in mmol/l: 415 NaCl, 10.2 KCl, 28 Na_2SO_4, 10 $CaCl_2$; pH = 8.0) containing 50 mmol/l $MgCl_2$ was added to the anterior compartment, and ASW containing 75 mmol/l $C_5H_{14}ClNO$ (choline chloride) was added to the posterior compartment for osmotic balancing. An additional group of hagfish was also placed into undivided chambers filled with Mg^{2+}-free seawater containing 75 mmol/l $C_5H_{14}ClNO$ to determine endogenously derived branchial, cutaneous, and cloacal Mg^{2+} flux into the Mg^{2+}-free solution. All solutions were osmotically balanced with mannitol (±1.0 mosmol/kg; VAPRO vapor pressure osmometer, model 5520; Wescor, Logan, UT). No detectable movement of Mg^{2+} from the anterior-to-posterior chamber over 4 h was observed, which ruled out any leakage between compartments (Mg^{2+} detection limit of 0.94 μmol/l).

Series 2: localization of routes of ammonia excretion following HEA. The effects of localized HEA exposure in anterior versus posterior body regions were determined by exposing each region individually to HEA and measuring ammonia flux in the other compartment. Hagfish were sampled for blood and placed in the divided chambers, followed by addition of sufficient NH_4Cl stock solution (1 mol/l prepared in autoclaved seawater) to either the anterior or posterior compartment to yield a $[T_{Amm}]$ of 20 mmol/l. Water samples were drawn immediately in the opposing compartment and again after 4 h, acidified, and stored at −20°C until further analysis. The animals were then removed and blood samples collected for pH and T_{Amm} measurement.

Series 3: skin as a route of ammonia excretion. Measurements of J_{Amm} were made on patches of skin using the method described by Glover et al. (26). Hagfish were held in ammonia-free seawater or exposed to HEA (20 mmol/l NH_4Cl) for 48 h and then killed by TMS overdose (as above). The skin, dorsal to slime glands running the

length of the body from the approximate fifth branchiopore to the tail, was removed, and five skin patches bisected by the dorsal midline (~3 cm × ~3 cm) were prepared. Samples of skin were also fixed for immunohistochemistry (see *Histology and immunohistochemical detection of EsRhcg in skin tissue*). Skin patches were maintained in aerated saline (in mmol/l: 474 NaCl, 8 KCl, 9 $MgCl_2$, 3 $MgSO_4$, 2.06 NaH_2PO_4, 5 $NaHCO_3$, 20 HEPES, and 5 glucose; pH = 7.8) and used within 1 h of excision. Each individual patch was placed over the top of the flux vial and secured in place with the serosal (basal) side of the skin facing outward. The inverted chamber was then placed in a small plastic bottle (serosal bath) containing 20 ml of hagfish saline containing different [T_{Amm}] (0.05, 0.1, 0.5, 1.0, 5.0 mmol/l). The inner chamber of the vial served as the mucosal bath and was composed of filtered, autoclaved seawater. Serosal and mucosal solutions were independently mixed using a pipette, and continual aeration was provided throughout the flux period whereby the direction of flux was from the serosal bath to the mucosal bath. Mucosal water samples (1 ml) were drawn at the beginning and end of each flux measurement period (0, 2 h). Water samples were then acidified as above and stored at −20°C until further analysis.

In a second set of experiments, the ammonia excretion capacity of the skin was determined along the length of the hagfish. Six patches of skin (~3 cm × ~3 cm) were excised as above at regular intervals (~12% of total body length) along the longitudinal axis of the body encompassing both anterior and posterior regions of the animal and tested for differences in J_{Amm}.

Series 4: role of Rh glycoproteins in ammonia excretion by Pacific hagfish. Multispecies alignments for Rh glycoprotein were constructed (15 Rhbg and 13 Rhcg homologues; Table 1) using MUSCLE (multiple sequence comparison by log - expectation; http://www.ebi.ac.uk/Tools/msa/muscle/) and an HMM (Hidden Markov model) profile for each isoform was determined using HMMER3 (version 3.0; Janelia Farm; hmmer.janelia.org). With these profiles, HMMER searches were conducted through a translated hagfish gill/slime gland Illumina transcriptome (12), and results were analyzed via BLAST (Basic Local Alignment Search Tool) on NCBI to verify Rh family homology. Searches resulted in a full-length sequence for Pacific hagfish Rhcg [*E. stoutii* Rhcg; including 5′ and 3′ untranslated regions (UTRs)] and two partial sequences for Rh-like (Rh-like; sequence 1 containing 5′-UTR and sequence 2 containing 3′-UTR). The previous designation of hRhcg (22) does not take into account the different genera and species of hagfish; thus we propose to term these newly cloned/sequenced Rh transcripts as *Es*Rhcg and *Es*Rh-like, and these isoform identities were confirmed via phylogenetic analysis (see RESULTS). With the use of this sequence information, PCR primers were constructed using the UTRs (Table 2) to confirm full-length coding sequence (CDS) via cloning (see *Molecular determination of EsRhcg and EsRh-like transcripts*).

Series 5: determination of cutaneous EsRhcg abundance along the length of the animal. Hagfish that were not previously exposed to experimental HEA were terminally anesthetized (as stated previously). Animals were then weighed and total animal length was recorded. Skin was excised at three locations (anterior, middle, and posterior) at measured lengths from the snout of the animal. Excised skin was immediately transferred to a 2-ml Eppendorf tube containing RNAlater. Samples were then stored at −20°C until protein expression analysis could be determined by electrophoresis and Western blot.

Table 1. *List of Rh protein sequences used for HMMER search*

Isoform	Species	Accession No.
Rhbg	*Takifugu rubripes*	AAM48577.1
	Alcolapia grahami	AFZ78445.1
	Cyprinus carpio	AGM46574.1
	Porichthys notatus	AGA93879.1
	Opsanus beta	AEA77168.1
	Bos taurus	AAI33319.1
	Rattus norvegicus	AAH79365.1
	Oryzias latipes	NP_001098561.1
	Danio rerio	NP_956365.2
	Takifugu rubripes	AAM48577.1
	Porichthys notatus	AGA93879.1
	Ophiophagus hannah	ETE58616.1
	Xenopus tropicalis	AAU89493.1
	Pan troglodytes	AAX39716.1
	Tetraodon nigroviridis	Q3BBX8.1
Rhcg	*Takifugu rubripes*	Q18PF5.1
	Danio rerio	NP_001083046.1
	Oncorhynchus mykiss	NP_001117995.1
	Oreochromis niloticus	XP_003440627.1
	Opsanus beta	AEA77169.1
	Gallus gallus	NP_001004370.1
	Monodelphis domestica	XP_001369976.1
	Xenopus tropicalis	NP_001003661.1
	Sus scrofa	NP_001038042.1
	Anolis carolinensis	XP_003227100.1
	Canis lupus familiaris	NP_001041487.1
	Pan troglodytes	NP_001030600.1
	Homo sapiens	NP_057405.1

Rh glycoprotein sequences used to construct hmm profiles for HMMER search querying hagfish illumina transcriptomes. Rhesus glycoprotein type c (Rhcg) and Rhesus glycoprotein type b (Rhbg) sequences were acquired from NCBI GenBank respository. See Table 2 for list of primers used for PCR amplification.

Table 2. *List of primers used for PCR amplification*

Application	Sequences
*Es*Rhcg	
PCR set Full CDS	Sense: 5′-CCTGCTGTATAACCGGTCGATATT-3′
	Antisense: 5′-CCAATGGAGCTTGCACCAAATA-3′
*Es*Rh-like	
PCR set Full CDS	Sense: 5′-CAACTCCGAGCTTCGCAA-3′
	Antisense: 5′-TGCCTGTATGTCTGCTTGTATG-3′

Analytical Methods

Blood sample analysis. Immediately following blood collection, blood pH was measured using a thermojacketed (10°C) Orion ROSS Micro pH electrode (Fisher Scientific, Ottawa, ON, Canada). The blood samples were then centrifuged (12,000 *g* for 30 s), and the plasma was stored at −80°C for T_{Amm} analysis. Plasma T_{Amm} concentration was quantified enzymatically using a commercial kit (Sigma-Aldrich Procedure A001) at 340 nm.

Water chemistry. Water ammonia concentrations were determined colorimetrically using the salicylate-hypochlorite assay at 650 nm (49), with a microplate spectrophotometer (Spectramax 190, Molecular Devices, Sunnyvale, CA) as previously described (14). Samples for Mg^{2+} quantification (*series 2*) were analyzed using an atomic absorption spectrophotometer (Thermo Scientific model iCE 3300).

Molecular determination of EsRhcg and EsRh-like transcripts. Total RNA was obtained from control hagfish gill (~100 mg) using TRIzol extraction. DNase I (Ambion/Life Technologies, Carlsbad, CA)-treated RNA was used to synthesize cDNA using RevertAid H-minus M-MuLV reverse transcriptase (Fermentas/Thermo Scientific, Pittsburgh, PA). PCR reactions targeting full-length CDS (coding DNA sequence) were conducted using Phusion DNA polymerase (Thermo Scientific, Pittsburgh, PA) with species-specific primers (Table 2) for 35 cycles. Amplicons were analyzed by gel electrophoresis, imaged using Alpha Imager 2200, and gel purified using QIAquick Gel Extraction Kit (cat. no. 28704). Products were cloned into *Eschericia coli* (dh5-α) using the CloneJet PCR cloning kit

(Thermo Scientific). Plasmid DNA was isolated and sequenced at the University of Alberta.

Phylogenetic sequence analysis of cloned EsRhcg and EsRh-like transcripts. An alignment of the sequenced hagfish Rh glycoprotein homologues against Rh homologues from other species was conducted using MUSCLE (21) in SeaView (25, 27) for MacOS. The resulting alignment was then refined using GBlocks (8) to subtract gaps and residues of low/noisy homology with parameters selected to allow for more relaxed stringency (47). Phylogenetic analysis was conducted on the Cyberinfrastructure for Phylogenetic Research (CIPRES) Science Gateway servers (37) using RAxML version 8.0.9 (45) utilizing the LG evolutionary model (33). Branch support was estimated by bootstrap with 300 replications (auto-cutoff set at 1,000 bootstraps). For phylogenetic analysis, base frequencies were model determined, and the proportion of invariable sites was determined using the GTRGAMMA model. A total of 85 protein sequences from the Rh glycoprotein family were collected from different species (including hagfish *Es*Rhcg and *Es*Rh-like protein sequences) and used in the analysis.

Histology and immunohistochemical detection of EsRhcg in skin tissue. Skin from non-HEA-exposed hagfish (*series 3* experiments) was placed in fixative (4% paraformaldehyde in 10 mmol/l phosphate-buffered saline, pH 7.4) for 24 h at 4°C, rinsed (3 times) in phosphate-buffered saline and then paraffin processed. Paraffin-processed tissue was sectioned at 7 μm on a Leitz microtome and mounted on positively charged slides (Fisher Scientific). Sections were blocked (5% normal goat serum and 0.1% Tween-20 in PBS at pH 7.4) and then incubated with primary antibody hagfish anti-hRhcg (α-hRhcg; 22), diluted in blocking solution (α-hRhcg; 1/500) overnight at room temperature, in a humidified chamber. Unbound primary antibody was removed by washing the sections in PBS. Sections were then incubated with Alexa Fluor goat anti-rabbit 568 (Molecular probes, Grand Island, NY) secondary antibody diluted in block for 1 h at RT. After being rinsied for 15 min in PBS, sections were coverslipped using Prolon gold antifade reagent (Invitrogen, Grand Island, NY) and visualized using a Zeiss LSM510 Confocal Microscope.

Negative staining controls for *Es*Rhcg were processed in the absence of primary antibody and using preabsorbed antibody incubations. In preabsorbed controls, α-hRhcg was diluted to 1.25 μg/ml in blocking solution containing 2.5 μg/ml of α-hRhcg antigen. The antibody and peptide mixture was incubated at RT for 30 min before addition to tissue sections. Routine hematoxylin and eosin staining was used for structural reference, using methods described by Weinrauch et al. (52).

Electrophoresis and Western blot analysis. Skin samples from *series 5* (stored in RNAlater) were pulverized under liquid nitrogen and then transferred (~100 mg) to a centrifuge tube containing 1:10 wt/vol of ice-cold homogenization buffer (250 mmol/l sucrose, 1 mmol/l EDTA, 30 mmol/l Tris, 100 mg/ml PMSF, and 5 mg/ml protease inhibitor cocktail). Samples were then homogenized on ice using a hand-held motorized mortar and pestle (Gerresheimer Kimble Kontes, Dusseldorf, Germany) for 45 s. Homogenates were then centrifuged at 3,000 *g* for 10 min at 4°C, and the supernatant was drawn off. A subsample of the supernatant was assayed for protein determination via the BCA (bicinchoninic) technique (Thermo Scientific).

Processed gill samples were diluted with 3× Laemmli buffer (31), and 25 μg of total protein were loaded in Criterion-TGX 20% acrylamide gels (Bio-Rad, Hercules, CA) and separated by sodium dodecyl sulfate, polyacrylamide gel electrophoresis (SDS-PAGE). Protein was transferred to a nitrocellulose membrane (Millipore, Billerica, MA). Protein transfer was confirmed by soaking membranes in Ponsceau S staining solution [0.1% (wt/vol) Ponceau S in 1% (vol/vol) acetic acid]. Membranes were washed (2 min in distilled water followed by 3 × 1 min in 0.5 M Tris-buffered saline [(TBS); pH = 8.0, containing 0.2% Tween-20 (TBST)] and then blocked in 5% blotto (5% skim milk powder in TBST) on a shaking carousel overnight at 4°C.

Membranes were washed (3 × 15 min in TBS and then 3 × 15 min in TBST) before overnight incubation in blocking buffer containing primary antibody (1:5,000 rabbit anti-*h*Rchg) at room temperature. Membranes were then washed three times (15 min in TBST) and incubated with secondary antibody (1:10,000 goat anti-rabbit horseradish peroxidase; Santa Cruz Biotechnologies, Dallas, TX) and Precision Protein StrepTactin-HRP conjugate (Bio-Rad) in TBST at room temperature for 1 h. Membranes were washed three times (15 min) in TBST followed by a final wash in TBS. Labeled protein bands were detected via enhanced chemiluminescence (ECL; Pierce; Super-Signal West Pico Chemiluminescent Substrate; Rockford, IL). Visualization occurred using Bio-Rad Chemidoc system with densitometry analysis completed using image analysis software (Bio-Rad). Standardization for protein concentration was quantified on the basis of 25 μg of total protein loaded into each well.

Calculations and Statistical Analysis

Calculations of J_{Amm} were based on the T_{Amm} accumulation in the water in either the anterior and/or posterior compartments using the following equation:

$$J_{Amm} = \left(\left[T_{Amm}\right]_{final} - \left[T_{Amm}\right]_{initial} \cdot V\right) \cdot \frac{1}{m} \cdot \frac{1}{\Delta t} \quad (1)$$

where $[T_{Amm}]$ is the initial or final concentration of ammonia in the water (μmol/l); V is the volume of water (ml); m is the animal mass (g), and Δt the duration of the flux period.

Rates of J_{Amm} across excised hagfish skin were determined by measuring ammonia appearance in the mucosal bath of the miniature flux chambers using the following equation:

$$J_{Amm}^{Skin} = \left(\left[T_{Amm}\right]_{final} - \left[T_{Amm}\right]_{initial} \cdot V\right) \cdot \frac{1}{SA} \cdot \frac{1}{\Delta t} \quad (2)$$

where SA is the measured mucosal surface area of hagfish skin exposed to seawater (cm^2), and other notations are as stated above.

When hagfish were placed in the divided chambers, ~40% of the hagfish skin was in the anterior compartment, whereas ~60% was in the posterior compartment. With this partitioning in mind, rough estimates of branchial and cutaneous J_{Amm} rates ($J_{Amm}^{branc}$and J_{Amm}^{cutan}, respectively) were calculated from experimentally determined average anterior and posterior rates (J_{Amm}^{ant} and J_{Amm}^{post}) as follows.

$$J_{Amm}^{cutan} = J_{Amm}^{post} + \left[\left(\frac{J_{Amm}^{post}}{60\%}\right) \cdot 40\%\right] \quad (3)$$

$$J_{Amm}^{branc} = J_{Amm}^{ant} - \left[\left(\frac{J_{Amm}^{post}}{60\%}\right) \cdot 40\%\right] \quad (4)$$

All data are presented as the means ± SE. Differences between groups with respect to plasma T_{Amm} and blood pH were tested using two-way analysis of variance (ANOVA) followed by Holm-Sidak's multiple comparison post hoc tests. Differences in J_{Amm} for the divided chamber studies during recovery from HEA exposure were tested using one-way ANOVA followed by Holm-Sidak's multiple comparison post hoc tests. Differences in plasma T_{Amm} in localized HEA exposure studies were tested using a Kruskal-Wallis nonparametric test followed by Dunn's multiple comparisons test, whereas differences in blood pH in this series were tested with one-way ANOVA followed by Holm-Sidak's multiple comparison post hoc test. Differences in anterior and posterior J_{Amm} in localized HEA-exposure experiments were tested with Student's one-tailed unpaired *t*-test with Welch's correction. Measurements of J_{Amm} across excised skin (skin from HEA vs. non-HEA hagfish) were compared using multiple Student's two-tailed *t*-test with a Holm-Sidak correction for

multiple comparisons. Differences in skin J_{Amm} along the hagfish length were tested for by linear regression analysis. Differences in *Es*Rhcg abundance along the length of the skin were tested using one-way ANOVA followed by Holm-Sidak's multiple comparison post hoc test. The fiducial limit of statistical significance was $P < 0.05$. All statistical analyses were completed using GraphPad Prism 6.0 (GraphPad Software, San Diego, CA).

RESULTS

Series 1: Sites of J_{Amm} After HEA Exposure

Plasma T_{Amm} was below the limit of detection in Pacific hagfish before HEA exposure and did not rise significantly in the parallel control animals not exposed to HEA. Exposure to 20 mmol/l total ammonia (HEA) for 48 h resulted in no mortalities but did lead to elevated plasma T_{Amm}, which increased to ~2,600 μmol/l ($P < 0.0001$; Fig. 1*A*). After HEA exposure, subsets of animals were then allowed to recover for 4 h in ammonia-free sea water in divided chambers, with half of the animals fitted with a cloacal seal. By 4 h of recovery, plasma T_{Amm} was significantly reduced by ~30–40% regardless of the presence of the cloacal seal ($P < 0.0001$; Fig. 1*A*).

In control (non-HEA exposed) hagfish, blood pH (Fig. 1*B*) was unchanged after HEA exposure ($P = 0.7816$) and was slightly elevated in the group of hagfish not fitted with the cloacal seal (Fig. 1*B*; $P = 0.0016$) but not in those animals fitted with the seal (no HEA; $P = 0.3920$; Fig. 1*B*). After 4 h of recovery in ammonia-free water, the hagfish with and without the cloacal seal experienced a slight metabolic acidosis characterized by respective reductions of 0.44 and 0.33 pH units, which were significantly lower than values measured immediately following HEA ($P < 0.0001$). It was notable that the control animals also underwent a slight metabolic acidosis following time-matched recovery in the divided chamber (~0.18 pH units; $P < 0.0001$).

When control hagfish not exposed to ammonia were placed in divided chambers, routine J_{Amm} averaged 40.0 ± 25.9 $\mu mol \cdot kg^{-1} \cdot h^{-1}$ (Fig. 2*A*) in the anterior compartment and 4.9 ± 1.4 $\mu mol \cdot kg^{-1} \cdot h^{-1}$ in the posterior compartment (Fig. 2*B*). However, recovery from 48 h exposure to HEA resulted in rates of anterior J_{Amm} that were significantly greater (~15-fold) compared with controls, in both those hagfish that were not fitted with the cloacal seal ($P = 0.0022$) and those that were ($P = 0.0022$; Fig. 2*A*). Excretion in the posterior compartment also increased significantly by ~30-fold in hagfish having no cloacal seal ($P < 0.0001$) and ~23-fold in those with the seal ($P < 0.0001$). No statistical differences in J_{Amm} were observed between animals with and without a cloacal seal in either the anterior ($P = 0.7279$) or posterior compartment ($P = 0.1358$). In HEA-exposed animals, the posterior excretion represented ~19% of the total J_{Amm} (combined anterior plus posterior) in animals with no cloacal seal and ~17% in animals with a cloacal seal compared with ~11% in the nonexposed controls (Fig. 2*B*).

Series 2: Localization of Routes of J_{Amm} After HEA

Exposure of the anterior region of the hagfish to HEA for 4 h resulted in a plasma T_{Amm} load of ~80 μmol/l but was not significantly different ($P = 0.5988$) compared with concentrations measured in control (no HEA) animals, which were below detectable limits (Fig. 3*A*). Notably, when the posterior

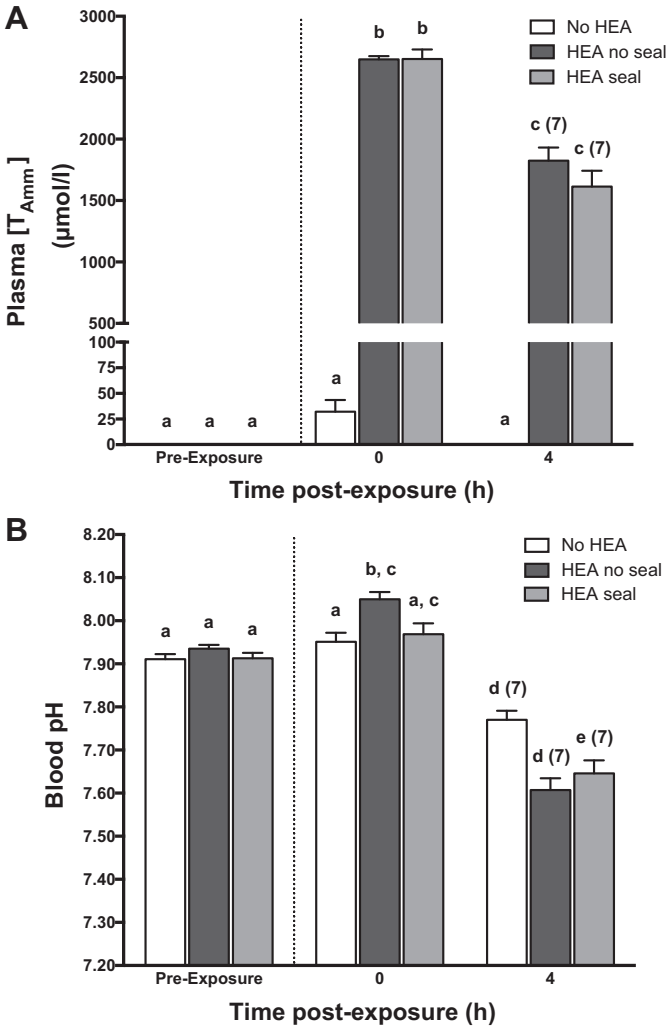

Fig. 1. Changes in plasma total ammonia concentration ([T_{Amm}]) (*A*) and blood pH (*B*) of Pacific hagfish exposed to high environmental ammonia (HEA) (closed bars; 20 mmol/l) for 48 h and after a 4-h recovery period in ammonia-free, full-strength seawater within divided chambers. Control fish (No HEA; open bars) were housed in ammonia-free seawater for the exposure period. Blood was drawn immediately before HEA exposure (Preexposure), after HEA exposure (0 h), and after a 4-h recovery period (4 h). After blood sampling was completed at 0 h, a subset of HEA-exposed hagfish were fitted with a cloacal seal (HEA seal; light gray bars), whereas the other group was left untreated (HEA no seal; dark gray bars) before being positioned into divided flux chambers. Data are presented as means + SE ($n = 8$) unless otherwise specified. Bars with same letter are not statistically different ($P < 0.05$) as determined by two-way ANOVA followed by Holm-Sidak's multiple comparisons post hoc test with all possible comparisons made.

end of the hagfish was exposed to HEA, animals experienced substantial (>1,500 μmol/l) accumulations in plasma T_{Amm} compared with both control ($P < 0.0001$) and anteriorly HEA-exposed hagfish (~21-fold greater; $P < 0.0074$; Fig. 3*A*).

While no differences in blood pH were observed after 4 h exposure of the anterior body to HEA compared with control animals ($P = 0.7484$), exposure of the posterior body regions to HEA resulted in a significant acidosis compared with anteriorly HEA-exposed animals characterized by a 0.3 pH unit drop ($P = 0.0443$; Fig. 3*B*).

When the route of HEA exposure was via either the anterior or posterior chamber, J_{Amm} was measured in the opposing

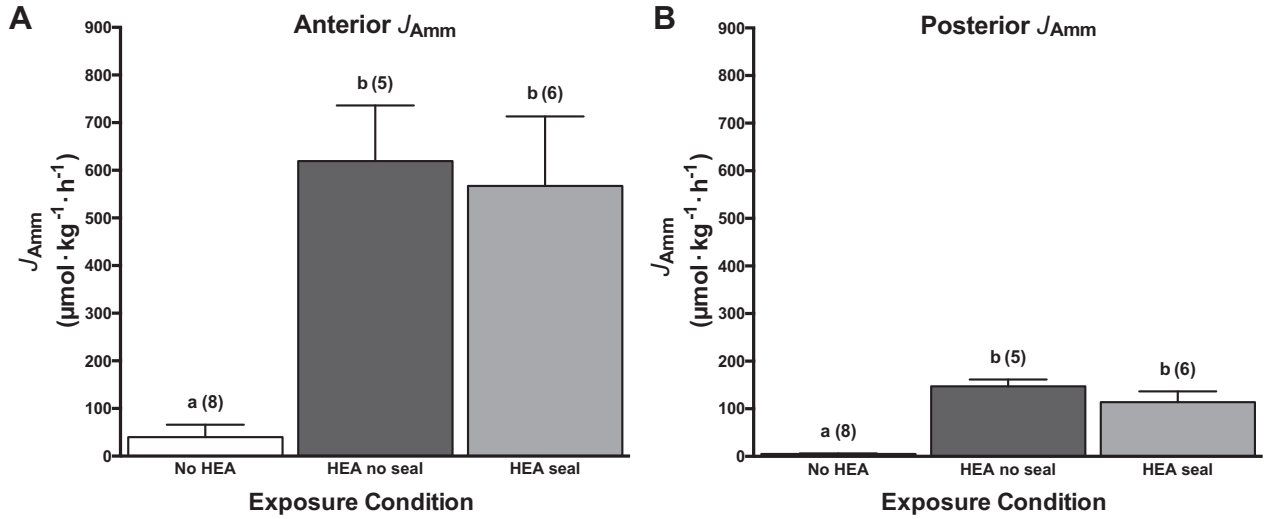

Fig. 2. Partitioning of net outward ammonia excretion (J_{Amm}) in Pacific hagfish exposed to HEA (20 mmol/l) for 48 h during recovery in ammonia-free, full-strength seawater within divided chambers. Control fish (No HEA; open bars) were housed in ammonia-free seawater for the duration of the exposure period. J_{Amm} was measured in the anterior (*A*) and posterior (*B*) chambers during the 4-h recovery period. Data are presented as means + SE (*n*). Bars with same letter are not statistically different ($P < 0.05$) as determined by one-way ANOVA followed by Holm-Sidak's multiple comparisons post hoc test. Details of cloacal seal application are described in Fig. 1.

HEA-free compartment. When HEA exposure was via the posterior compartment, anterior J_{Amm} was ~4-fold greater than anterior rates in control animals ($P = 0.0329$; Fig. 4*A*). When the route of HEA was via the anterior compartment, posterior J_{Amm} was ~25-fold greater than that measured in controls ($P = 0.0085$; Fig. 4*B*).

Series 3: Ammonia Flux Across Excised Skin Tissue

To further investigate the skin's role in ammonia handling, skin patches were excised from the dorsal region of hagfish exposed to HEA (20 mmol/l) for 48 h or from control animals held in ammonia-free seawater. In both cases J_{Amm} was measured while the serosal side of the patches was exposed to a range of serosal T_{Amm} concentrations. When compared with the controls, J_{Amm} was significantly greater in skin patches excised from HEA-exposed hagfish at all but the highest T_{Amm} concentrations (10 mmol/l; $P = 0.1786$); notably, J_{Amm} across the skin excised from HEA-exposed animals was ~8-fold greater at a serosal [T_{Amm}] of 0.05 and 0.1 mmol/l ($P = 0.0006$ and $P = 0.0135$, respectively), ~4-fold greater at 0.5 and 1.0 mmol/l ($P = 0.0027$ and $P = 0.0026$, respectively), and 1.3-fold greater at a serosal [T_{Amm}] of 5 mmol/l ($P = 0.0434$; Fig. 5*A*).

The skin contribution to J_{Amm} also appeared to be greater in posterior relative to anterior body regions, with J_{Amm} increasing linearly in skin sections sampled sequentially from anterior to posterior ($R^2 = 0.88$) with a slope of 0.1307 ± 0.024 [(nmol·cm^{-2}·h^{-1})/(% distance from snout)] that was significantly different from a slope of 0 ($F_{1,4} = 30.30$, $P = 0.0053$l) and an intercept of 18.82 ± 1.436 nmol·cm^{-2}·h^{-1} (Fig. 5*B*).

Series 4: Detection and Distribution of EsRhcg in Cutaneous Tissue

With the use of an Illumina transcriptome for combined gill/slime gland, a full-length sequence for *Es*Rhcg and a partial *Es*Rh-like sequence were isolated. With the use of species-specific primers generated from transcriptomic data, full-length amplicons were amplified using PCR. Sequencing following subsequent cloning identified a 1,386 bp ORF (open reading frame) encoding a 462 amino acid residue protein for *Es*Rhcg sequence and a 1,443 bp ORF encoding a 481 amino acid protein for *Es*Rh-like sequence. These sequences share high homology (>98% at amino acid level) with previously identified homologues from Atlantic hagfish (22). Maximum likelihood phylogenetic analysis of these sequences against subfamilies of the Rh glycoprotein family demonstrated that the cloned *Es*Rhcg and *Es*Rh-like are members of the Rh glycoprotein family (Fig. 6). Full-length sequences for cloned *Es*Rhcg and *Es*Rh-like sequences are found on the NCBI database (accession numbers KT943755, KT943754, respectively).

Hematoxylin and eosin staining highlighted the cellular composition of the capillary (Cp)-rich dermis (De) (20, 28, 32, 39, 53), as well as the prominent mucous cells (MC) in the basal aspect of the epidermis (Ep; Fig. 7*A*). Immunohistochemical analysis, using α-hRhcg antibody (22), demonstrated that *Es*Rhcg immunoreactivity was more prominently localized toward the basal aspect of the skin epidermis but not in the dermal layer (Fig. 7*B*). Peptide competition eliminated this staining in the epithelial layer but not the nonspecific staining in the dermal layer (Fig. 7*B*, *inset*). The Pacific hagfish *Es*Rhcg sequence exhibited 88% (15/17 amino acids) identity with the antigenic peptide sequence used to create α-hRhcg antibody (Table 3).

Series 5: Determination of Relative Cutaneous EsRhcg Abundance Along the Length of the Animal

Skin tissue excised sequentially from anterior to posterior was distributed on a percentage distance from snout basis (anterior: $27.58 \pm 0.9\%$; middle: $57.21 \pm 1.40\%$; posterior: $84.19 \pm 1.08\%$). Western blot analysis on skin tissue using hagfish specific α-hRhcg antibody (22) yielded a single immu-

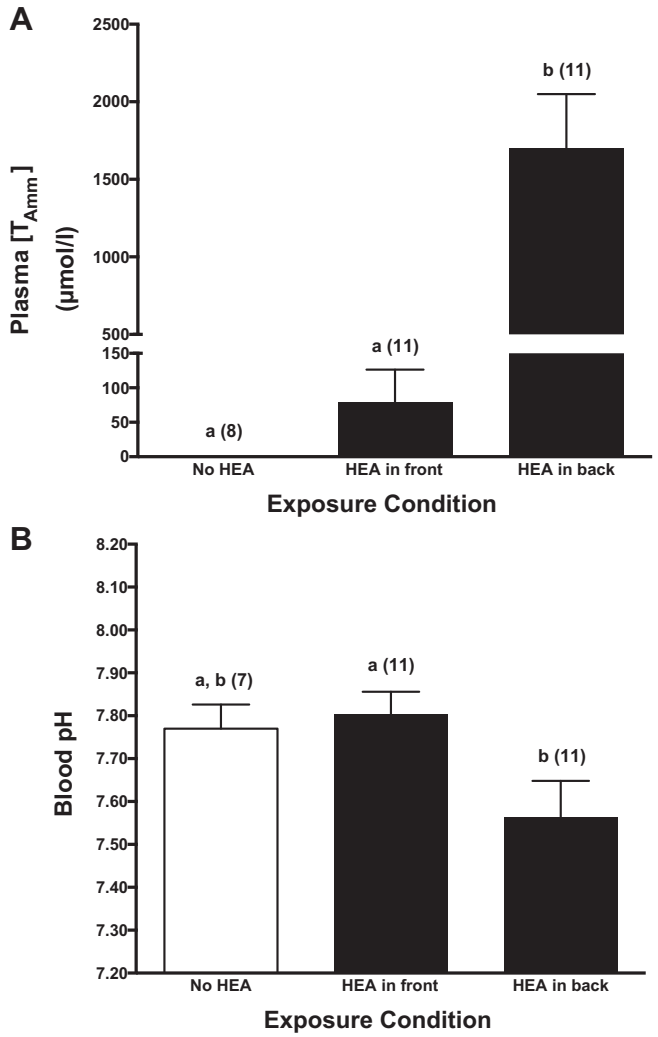

Fig. 3. Changes in plasma [T_{Amm}] (*A*) and blood pH (*B*) during localized exposure of hagfish to HEA (20 mM) via either ammonia-free seawater (no HEA; open bars) or 20 mmol/l T_{Amm} in either the anterior compartment (HEA in front) or the posterior compartment (HEA in back) divided chamber. Blood samples were drawn immediately after the 48-h exposure. Data are presented as means + SE (*n*). Bars with same letter are not statistically different ($P < 0.05$) as determined by a Kruskal-Wallis nonparametric test followed by Dunn's multiple comparison test in *A* and by one-way ANOVA followed by Holm-Sidak's multiple comparisons post hoc test in *B*.

noreactive protein band at ~50 kDa (duplicate representative blot of each skin section shown in Fig. 8*A*). Abundance of *Es*Rhcg was variable across the length of the skin and was statistically greater in skin sections excised from the middle of the trunk ($P = 0.0448$) and demonstrated an increasing trend in the posterior ($P = 0.0707$) sections of the animal compared with anterior sections (Fig. 8*B*). No significant differences were observed between the middle and posterior sections ($P = 0.6677$).

DISCUSSION

Hagfish have impressive capabilities to tolerate and excrete ammonia during HEA exposure (4, 14, 22, 23, 36). The present study demonstrates that following HEA exposure, hagfish excrete ammonia using both the gills and the skin. These findings are supported by the ~15-fold and ~23- to 30-fold greater rates of ammonia excretion that were observed in the anterior and posterior sections, respectively, of the animals following exposure to HEA for 48 h. Moreover, measurements of ammonia excretion on isolated skin patches demonstrated that the ammonia permeability of the skin increased along the length of the animal from anterior to posterior. Using immunocytochemistry, we also demonstrated that *Es*Rhcg is expressed in the epidermal layer of the skin of Pacific hagfish. This finding, taken together with our observation that *Es*Rhcg proteins were located immediately adjacent to the dermal capillaries, provides mechanistic evidence for ammonia transport via the skin. Differences in anterior and posterior J_{Amm} in localized ammonia exposure experiments matched the measured increases in J_{Amm} noted in more posterior skin sections in isolated skin flux studies. Importantly, these results also coincided with greater *Es*Rhcg expression in the middle and a trend ($P = 0.0707$) toward increased expression in posterior

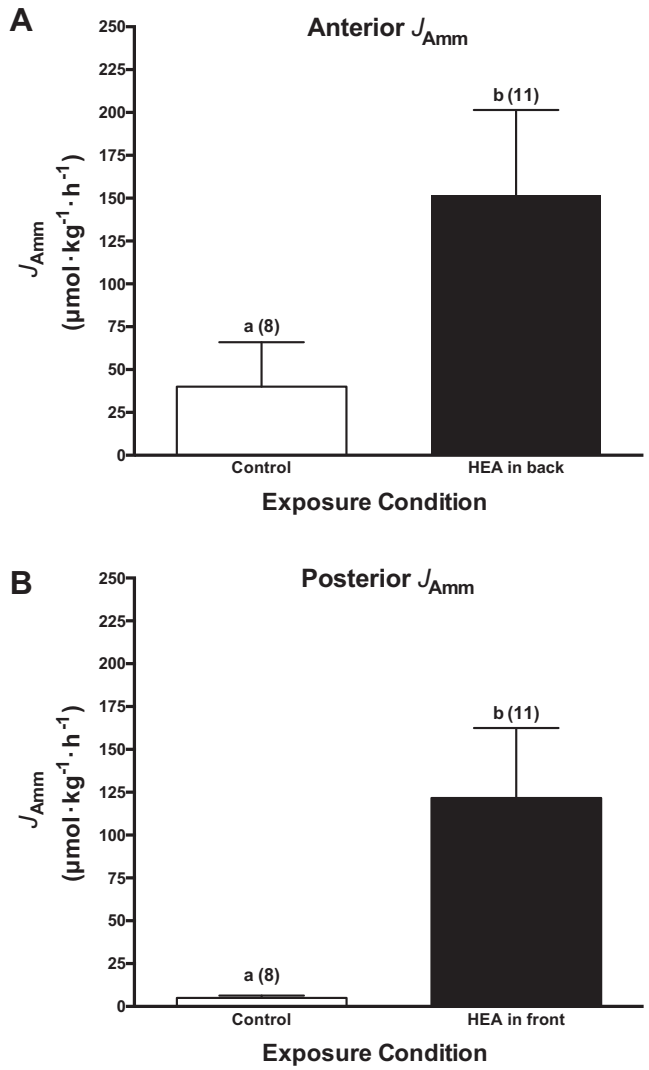

Fig. 4. Ammonia excretion during localized HEA exposure. Net outward anterior (*A*) and posterior (*B*) J_{Amm} from hagfish during acute localized HEA exposure was determined in the compartment opposite to the HEA-containing compartment. Data are presented as means + SE (*n*). Bars with same letter are not statistically different ($P < 0.05$) as determined by Student's one-tailed *t*-test.

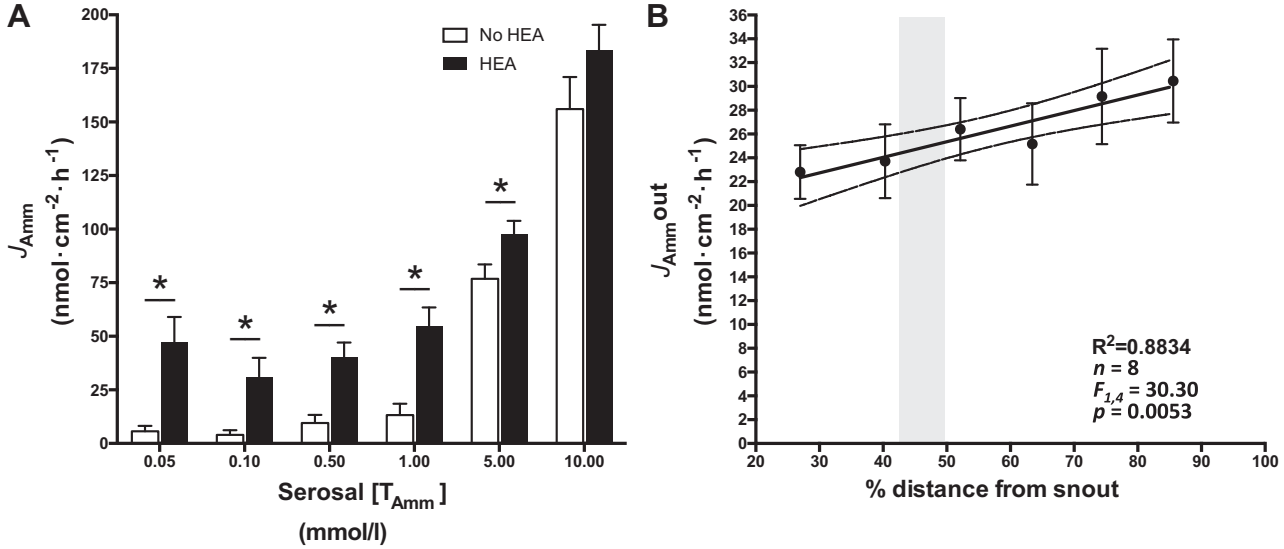

Fig. 5. Total ammonia flux across excised skin as determined by appearance of ammonia in mucosal medium following introduction to serosal HEA (0.05–10.0 mmol/l in hagfish saline). Concentration-dependent flux (*A*) was determined in excised skin from hagfish ($n = 6$) either preexposed to HEA (20 mmol/l) for 48 h (closed bars) or nonexposed controls (open bars). Skin J_{Amm} was measured in skin excised from serial sections along the length of non-HEA-exposed animals. The serosal side of skin sections was then exposed to 5 mmol/l T_{Amm} in hagfish saline, and the appearance of ammonia was measured on the mucosal side of the chamber. Data are presented as means + SE in *A* and means ± SE in *B*. Statistical differences in *A* (*$P < 0.05$) as determined by multiple Student's *t*-tests with a Holm-Sidak multiple comparisons correction. Solid line in *B* represents line of best fit as determined by linear regression analysis {equation: skin $J_{Amm} = 0.1307$ [(nmol·cm^{-2}·h^{-1})/(% distance from snout)] + 18.82 nmol·cm^{-2}·h^{-1}}; broken lines represent 95% confidence limits for line of best fit, and the shaded area represents the placement of collar assembly on hagfish in separating chamber protocols.

excised skin segments compared with anterior segments. We conclude that hagfish not only have the ability to differentially handle ammonia using both the gills and the skin, but also that the relative capacity of each route to excrete ammonia can be altered during and after exposure to HEA.

Ammonia excretion across the gills and the skin likely involves Rhesus glycoproteins, as described in other fish species (57). This interpretation is supported by the identification of two Pacific hagfish Rh orthologs of the SLC42 family of transporters. Comprehensive phylogenetic analysis demonstrates that two orthologs are confidently rooted within the well-conserved Rh transport family. These two *Eptatretid* Rhs (*Es*Rhcg and *Es*Rh-like) plus the two previously identified *Myxinid* Rhs (hRhcg and hRhbg, respectively) represent the earliest Rh proteins characterized in the extant vertebrate lineage. *Es*Rhcg clearly grouped with other Rhcg family members at the basal node for all other Rhcg homologues. A second sequence, defined as *Es*Rh-like, could not be attributed to either the Rhag or Rhbg family, but it did group with low confidence with Rh30-like proteins found in other teleost genomes.

Atlantic hagfish (*Myxine glutinosa*) express hRhcg not only in the gills, a common site for ammonia excretion, but also in skin (22). The presence of an extensive dermal capillary network (20, 28, 32, 39, 53) in hagfish skin is purported to be an important site of gas exchange (39); although, this hypothesis has been challenged based on the thickness of the skin (34) and a recent study clearly showing that Pacific hagfish lack the ability to cutaneously take-up sufficient O_2 to satisfy routine metabolic demands (16). In the current study, *Es*Rhcg was localized in the epidermal tissue in close proximity (≤20 μM; Fig. 7, *A* and *B*) to the dermal capillaries in Pacific hagfish. Because NH_3 is a much smaller molecule and ~10,000 times more soluble in water than oxygen (3, 5), we hypothesize that *Es*Rhcg in hagfish and its proximity to the dermal capillaries provide a mechanism for facilitated transport of ammonia across the skin that is not available for the transport of oxygen. The increasing permeability to ammonia along the length of the skin from the anterior to posterior regions of the hagfish (Fig. 5*B*) also supports this hypothesis.

Based on our observations, we propose that during feeding, the more posterior regions of hagfish skin have more favorable NH_3 diffusion gradients compared with the anterior regions, which may be buried in the carrion upon which the hagfish are feeding. During feeding events, there could be much higher concentrations of ammonia in the adjacent water near the anterior (head plus gills) regions due to decomposition of the carrion tissue and the more confined space, than in the more posterior regions, which are more distal to the carrion. The posterior regions also appear to be more ammonia permeable than the anterior regions, which may limit ammonia uptake via the gills/head region while simultaneously promoting offloading via the posterior regions while immersing themselves in their meals. Indeed, localized ammonia exposures demonstrate anterior (i.e., branchial) HEA exposure results in substantially less accumulation of plasma T_{Amm} (Fig. 3*A*) than does equivalent posterior HEA exposure. In contrast, the rise in plasma ammonia, when the route of exposure is via the posterior chamber, indicates that hagfish are less able to limit posterior cutaneous ammonia uptake, at least acutely. While the mechanisms behind the differences in the permeability of the anterior versus posterior regions of the hagfish remain unresolved, changes in gill ammonia permeability due to changes in *Es*Rhcg abundance can be ruled out. Western blots of gill tissue demonstrated that prolonged exposure of hagfish to identical ammonia concentrations used in the

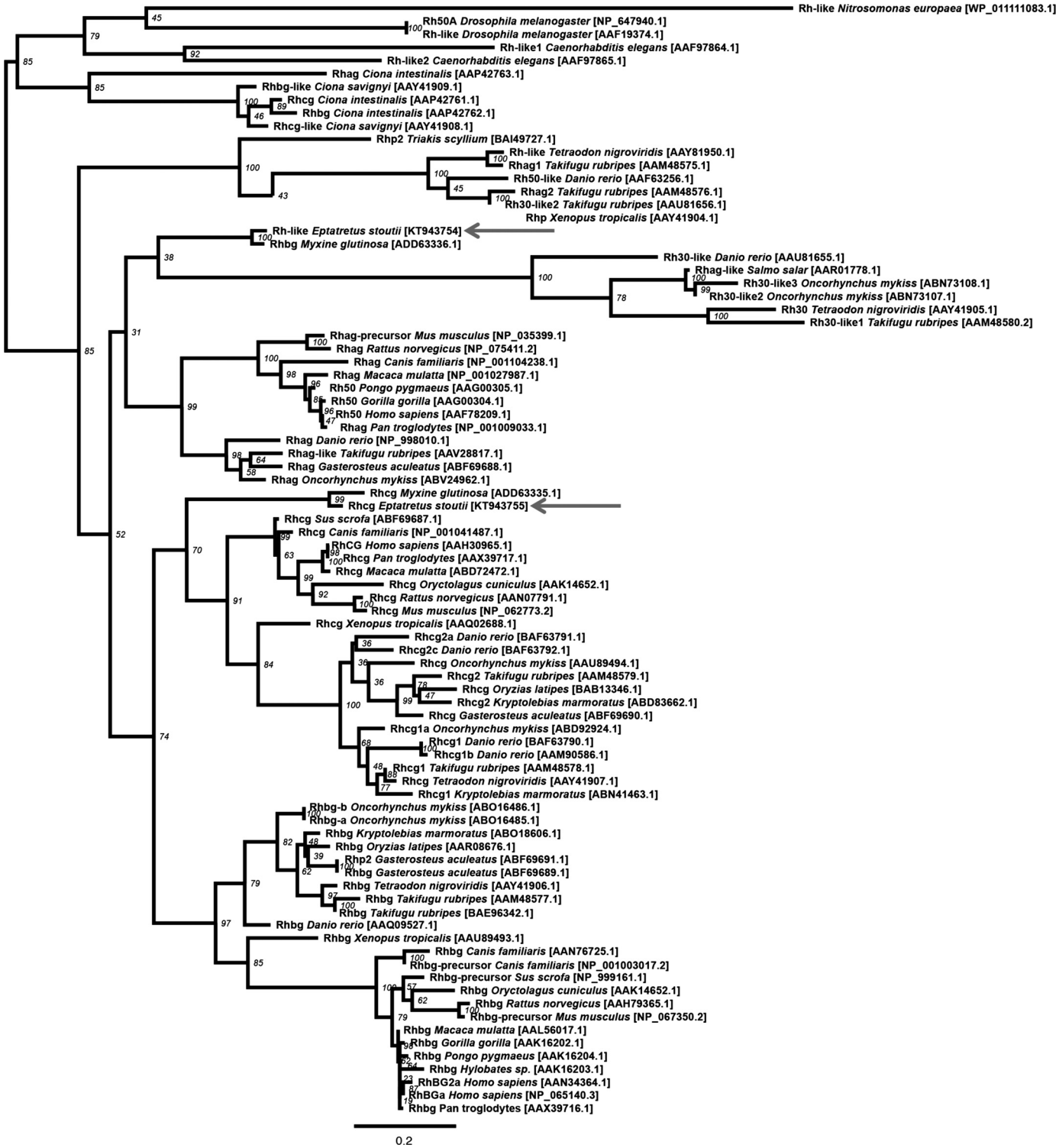

Fig. 6. Phylogenetic analysis of 2 cloned hagfish Rh glycoprotein sequences showed phylogenetic relationships of *Es*Rhcg and *Es*Rh-like peptide sequences. Analysis was completed using RAx-ML with methods previously described on the Cyberinfrastructure for Phylogenetic Research (CIPRES) Science Gateway servers. Branch support was estimated by bootstrap with 300 replications with auto-cutoff threshold set to 1,000. Cloned sequences are denoted with an arrow. Numbers in square brackets are the GenBank accession numbers of the sequences.

current study were not accompanied by changes of branchial *Es*Rhcg protein abundance (14).

Our results also demonstrate that regional differences in the cutaneous permeability to NH_3 may promote ammonia excretion in the posterior (cutaneous) regions of the hagfish when the anterior portions of its body are immersed in carrion during feeding (Fig. 4*B*). Presumably, the posterior portion of the animal would face lower environmental ammonia compared

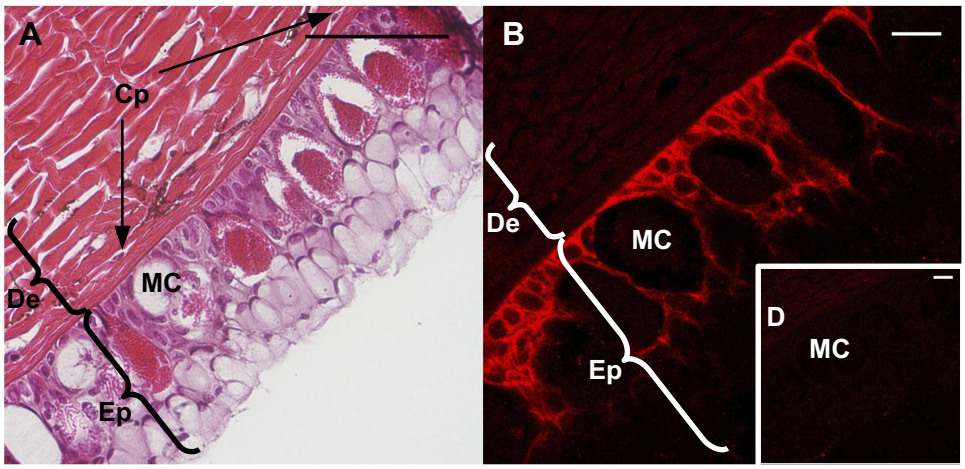

Fig. 7. Representative micrographs depicting Pacific hagfish cutaneous cellular organization and *Es*Rhcg localization. Hematoxylin and eosin staining (*A*) highlighting the large mucous cells (MC) and clearly defined basement membrane separating the epidermis (Ep) from the capillary-rich (Cp; denoted by arrows) dermis (De). Immunohistochemistry representative confocal images showing localization of the *Es*Rhcg using *Myxinid*-derived antibodies (red) to the basal aspect of the epidermis (*B*). Immunoreactivity was observed along the length of the basement membrane of the epidermis, extending up to surround the large MC. Preabsorbed antibody control micrograph (*B*, *inset)* demonstrating no evidence of *Es*Rhcg staining. Scale bars = 100 μm in *A* and 20 μm in *B*.

with the anterior portion in a feeding hagfish, which would facilitate a "flow-through" of ammonia from the anterior to the posterior of the animal. Unfortunately, reliable protein extracts could not to be obtained from frozen skin tissue from HEA and control fish. However, there were differences in *Es*Rhcg expression along the length of the animal with lower expression in anterior tissue and greater expression in skin excised from the middle and arguably, the posterior (see above) sections of the animal.

As facilitated transporters, Rh glycoproteins promote ammonia transport in a bidirectional manner along prevailing NH_3 partial pressure gradients (6, 51). Such bidirectional transport would be compatible with our proposed flow-through model. Under normal conditions, the anterior portions of the unrestrained (free swimming) hagfish would facilitate the bulk of ammonia excretion. When hagfish are immersed in carcasses during feeding, however, the posterior regions would take on added importance to unload ammonia that was inadvertently taken up from the carcass itself or the surrounding environment. Other factors including the extent of vascularization and local blood flow could also affect delivery and the relative permeability of the skin and gills to ammonia and should also be examined to determine how/if these processes are modulated. Nevertheless, the presence of *Es*Rhcg and its differential expression supports a substantive role for the skin and posterior regions of the animal.

Regional Differences in J_{Amm} After HEA Exposure

During recovery in sea water following ammonia exposure, both the gill and skin contributed to J_{Amm} in the anterior compartment, whereas cutaneous and cloacal (intestinal and renal combined) constituents contributed to J_{Amm} in the posterior compartment. Our experiments revealed that a cloacal seal did not impact J_{Amm} in the posterior chamber in either control (15) or HEA-exposed animals (Fig. 2*A*), demonstrating that cloacal efflux does not play a prominent role in J_{Amm}. Given the low urine flow rate of the hagfish (227 $\mu l \cdot kg^{-1} \cdot h^{-1}$; Ref. 38), the urine would have to be concentrated to >800 mmol/l to account for the measured J_{Amm}. This would be approximately two orders of magnitude greater than the hagfish plasma T_{Amm} following HEA exposure. Given that hagfish are osmoconformers (19), have rudimentary kidneys (52), and

Table 3. *Comparison of hagfish Rhcg antibody binding domain*

Species	Peptide Sequence
Myxine glutinosa	5′-CYEDRAYWEVPEEEVTY-3′
Eptatretus stoutii	5′-CYED**E**AYWEVPEEEVT**L**-3′

Species specific peptide sequence identity of hagfish Rhcg antibody binding domain. Differences in peptide identity between species isoforms are denoted in boldface.

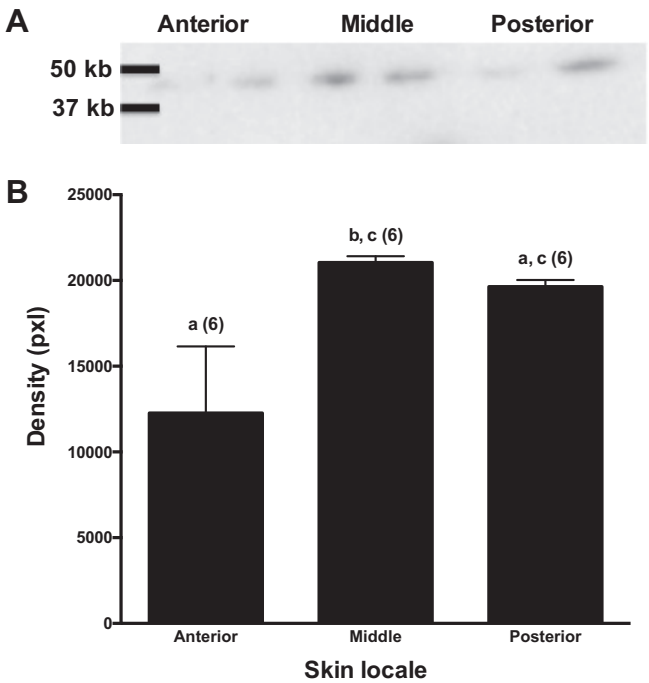

Fig. 8. Cutaneous distribution of *Es*Rhcg abundance in hagfish. Hagfish skin was excised in sequential sections (anterior, middle, posterior) from along the length of the animal. Skin sections were distributed by percentage distance from the snout (anterior: 27.58 ± 0.9%; middle: 57.21 ± 1.40%; posterior: 84.19 ± 1.08%). *A*: representative blot from anterior, middle, and posterior skin sections. *B*: relative abundance of cutaneous *Es*Rhcg expression from sequential skin sections. Data are presented as means + SE (*n*). Bars with same letter are not statistically different ($P < 0.05$) as determined by one-way ANOVA followed by Holm-Sidak's multiple comparisons post hoc test.

have a urine composition similar to plasma (1), it is unlikely that hagfish concentrate ammonia within their urine as a means of excretion; thus, posterior flux rates we measured are interpreted as being primarily cutaneous.

Currently, there are no estimates of branchial (gill pouch) surface area in hagfish, therefore, we are unable to empirically attribute flux of ammonia to either the skin or the gill surface area. Estimation of gill ammonia permeability is further complicated by the fact that there is considerable interspecies variation in the number of gill pouch pairs in *E. stoutii* (10–13 pairs; Ref. 52) and other hagfishes (40). Furthermore, it is unknown whether individual gill pouches along the length of the branchial region similarly express *Es*Rhcg. For these reasons, we only refer to anterior versus posterior flux contributions with the anterior portion obviously comprising both cutaneous and branchial components, whereas the posterior region only being composed of cutaneous exchange. Clearly, estimates of gill surface area and investigations of the branchial Rh profile in hagfishes are required to accurately attribute ammonia permeability to specific branchial versus cutaneous contributions. That said, adjusting for the presence of skin in the anterior chamber (see MATERIALS AND METHODS), rough estimates of cutaneous contributions to ammonia excretion were ~18% of total routine rates and increased to ~30% after exposure to HEA. Given the dynamic *Es*Rhcg profile and the changing J_{Amm} profile along the length of hagfish skin and the arguments listed above, these estimates should be cautiously interpreted. Cutaneous ammonia excretion has been observed in several fish species including dab (*Limanda limanda*; 41), rainbow trout (*Oncorhynchus mykiss*; 58), and the mangrove killifish (*Kryptolebian marmoratus*; 24). In trout, cutaneous ammonia excretion accounted for 4.5% of total J_{Amm} under routine conditions and mildly increased to 5.7% following HEA exposure (12 h; 2 mmol/l; 58), whereas in the dab, cutaneous ammonia excretion accounted for 47% under routine conditions; however, the effect of ammonia loading via HEA exposure in dab has yet to be determined (41).

Acid/Base Response During Exposure, Recovery, and Localized Exposure

Exposure to high environmental ammonia is known to result in a metabolic alkalosis (elevated pH), which is compensated for over the next 12 h by a compensatory retention of metabolic H^+ (56). However, during recovery in ammonia-free seawater, ammonia (NH_3) leaves preferentially and the result is an internal metabolic H^+ load (lowered pH) due to dissociation of NH_4^+ into NH_3 and H^+. Clifford et al. (14) reported a similar response in whole hagfish during similar HEA exposure; however, a perplexing result in the current study is the ~0.2 pH unit acidosis that was only observed following acute (4 h) posterior exposure to HEA and not with anteriorly applied HEA. Posterior entry of NH_4^+ could account for this result. However, the entry of ammonia as NH_4^+ seems unlikely given the relatively low cationic permeability of the hagfish body surface (23). Current understanding of Rh-facilitated ammonia transport based on mammalian Rh isoforms expressed in *Xenopus laevis* oocytes suggests that Rhcg only transports neutral NH_3 and is then trapped as NH_4^+ by H^+ excreted via branchial V-ATPases and/or NHE proteins (57). However, Caner et al. (6) also suggests that other isoforms of Rh protein (Rhbg, RhAG) are capable of transporting both neutral NH_3 and ionized NH_4^+ (6). The transporting capabilities of these hagfish isoforms with respect to substrate selectivity remain to be elucidated and provide avenues for future research with studies similar to those conducted by Caner et al. (6). A second possible explanation for the perplexing 0.2 pH unit acidosis still present after 4 h of posteriorly applied HEA is that the signal for acid-base regulation is branchially located and not stimulated by either posterior HEA application or elevated plasma ammonia. Clearly, the possibility of differentially activating acid-base regulatory responses by differential HEA application is intriguing and bears further investigation.

Perspectives and Significance

This study demonstrates that there is regional variation in ammonia transport in the hagfish and that the posterior regions of the hagfish may take on added importance when the anterior regions are exposed to high concentrations of ammonia, as could possibly occur when they are feeding on carrion. The expression of *Es*Rhcg protein in the epidermal tissue provides a mechanism by which ammonia can be transported across the thick epidermal layer that characterizes the trunk/posterior regions of the body. Furthermore, HEA-induced plasma ammonia loading results in a higher cutaneous permeability in excised skin suggesting that Pacific hagfish are able to differentially regulate the ammonia permeability of the gills and the skin. These adaptations may allow the hagfish to unload ammonia that is inadvertently taken-up by the gills while feeding on decaying carrion while simultaneously facilitating off-loading ammonia to the water via the skin in the more posterior regions of their body. Further investigation is necessary to identify the underlying mechanism responsible for this remarkable ability to limit ammonia uptake.

ACKNOWLEDGMENTS

We thank Dr. Eric Clellend (Research Coordinator at BMSC) for his unwavering diligence in supporting this research, Rachel Munger for assistance in sample collection, and Sam Guffey, Chris Wood, and Alex Zimmer for advice.

GRANTS

A. M. Clifford was supported by a Natural Sciences and Engineering Council of Canada (NSERC)-Postgraduate Scholarship-Doctoral (PGS D) (370386) and Alberta Innovates Technology Futures studentship grant; The Andrew Stewart Memorial prize; The Donald M. Ross scholarship and R. E. Peter Memorial Scholarship; The Western Canadian Universities Marine Sciences Society Graduate Student Award; and the Dick & Leona BMSC residential Bursary. G. G. Goss (203736) and M. P. Wilkie (194686) are supported by NSERC Discovery Grants. S. L. Edwards is supported by the National Science Foundation Grant: Integrative Organismal Systems (1121369).

DISCLOSURES

No conflicts of interest, financial or otherwise, are declared by the author(s).

AUTHOR CONTRIBUTIONS

A.M.C. and G.G.G. conceived and designed research; A.M.C., A.M.W., and S.L.E. performed experiments; A.M.C. and S.L.E. analyzed data; A.M.C., S.L.E., M.P.W., and G.G.G. interpreted results of experiments; A.M.C., A.M.W., and S.L.E. prepared figures; A.M.C. drafted manuscript; A.M.C., A.M.W., S.L.E., M.P.W., and G.G.G. edited and revised manuscript; A.M.C., A.M.W., S.L.E., M.P.W., and G.G.G. approved final version of manuscript.

REFERENCES

1. **Alt JM, Stolte H, Eisenbach GM, Walvig F.** Renal electrolyte and fluid excretion in the Atlantic hagfish *Myxine glutinosa*. *J Exp Biol* 91: 323–330, 1981.
2. **Bardack D.** First fossil hagfish (myxinoidea): a record from the pennsylvanian of illinois. *Science* 254: 701–703, 1991. doi:10.1126/science.254.5032.701.
3. **Boutilier RG, Heming TA, Iwama GK.** Appendix: physicochemical parameters for use in fish respiratory physiology In: *Gills–Anatomy, Gas Transfer, and Acid-Base Regulation*, edited by Hoar WS, Randall D. Orlando, FL: Elsevier, 1984, p. 403–430. doi:10.1016/S1546-5098(08)60323-4.
4. **Braun MH, Perry SF.** Ammonia and urea excretion in the Pacific hagfish *Eptatretus stoutii*: evidence for the involvement of Rh and UT proteins. *Comp Biochem Physiol A Mol Integr Physiol* 157: 405–415, 2010. doi:10.1016/j.cbpa.2010.08.020.
5. **Cameron JN, Heisler N.** Studies of ammonia in the Rainbow trout: Physico-chemical parameters, acid-base behaviour and respiratory clearance. *J Exp Biol* 105: 107–125, 1983.
6. **Caner T, Abdulnour-Nakhoul S, Brown K, Islam MT, Hamm LL, Nakhoul NL.** Mechanisms of ammonia and ammonium transport by rhesus-associated glycoproteins. *Am J Physiol Cell Physiol* 309: C747–C758, 2015.
7. **Carter DO, Yellowlees D, Tibbett M.** Cadaver decomposition in terrestrial ecosystems. *Naturwissenschaften* 94: 12–24, 2007. doi:10.1007/s00114-006-0159-1.
8. **Castresana J.** Selection of conserved blocks from multiple alignments for their use in phylogenetic analysis. *Mol Biol Evol* 17: 540–552, 2000. doi:10.1093/oxfordjournals.molbev.a026334.
9. **Chew SF, Jin Y, Ip YK.** The loach *Misgurnus anguillicaudatus* reduces amino acid catabolism and accumulates alanine and glutamine during aerial exposure. *Physiol Biochem Zool* 74: 226–237, 2001. doi:10.1086/319663.
10. **Chew SF, Wong MY, Tam WL, Ip YK.** The snakehead *Channa asiatica* accumulates alanine during aerial exposure, but is incapable of sustaining locomotory activities on land through partial amino acid catabolism. *J Exp Biol* 206: 693–704, 2003. doi:10.1242/jeb.00140.
11. **Clark AJ, Summers AP.** Morphology and kinematics of feeding in hagfish: possible functional advantages of jaws. *J Exp Biol* 210: 3897–3909, 2007. doi:10.1242/jeb.006940.
12. **Clifford AM, Bury NR, Schultz AG, Ede JD, Goss BL, Goss GG.** Regulation of plasma glucose and sulfate excretion in Pacific hagfish, *Eptatretus stoutii* is not mediated by 11-deoxycortisol. *Gen Comp Endocrinol* 247: 107–115, 2017. doi:10.1016/j.ygcen.2017.01.022.
13. **Clifford AM, Goss GG, Roa JN, Tresguerres M.** Acid/base and ionic regulation in hagfish. In: *Hagfish Biology*, edited Edwards SL, Goss GG. Boca Raton, FL: CRC, 2015, p. 277–298. doi:10.1201/b18935-12.
14. **Clifford AM, Goss GG, Wilkie MP.** Adaptations of a deep sea scavenger: High ammonia tolerance and active NH_4^+ excretion by the Pacific hagfish (*Eptatretus stoutii*). *Comp Biochem Physiol A* 182: 64–74, 2015. doi:10.1016/j.cbpa.2014.12.010.
15. **Clifford AM, Guffey SC, Goss GG.** Extrabranchial mechanisms of systemic pH recovery in hagfish (*Eptatretus stoutii*). *Comp Biochem Physiol A Mol Integr Physiol* 168: 82–89, 2014. doi:10.1016/j.cbpa.2013.11.009.
16. **Clifford AM, Zimmer AM, Wood CM, Goss GG.** It's all in the gills: evaluation of O2 uptake in Pacific hagfish refutes a major respiratory role for the skin. *J Exp Biol* 219: 2814–2818, 2016. doi:10.1242/jeb.141598.
17. **Collins MA, Yau C, Nolan CP, Bagley PM, Priede IG.** Behavioural observations on the scavenging fauna of the Patagonian slope. *J Mar Biol Assoc UK* 79: 963–970, 1999. doi:10.1017/S0025315499001198.
18. **Cox GK, Sandblom E, Richards JG, Farrell AP.** Anoxic survival of the Pacific hagfish (*Eptatretus stoutii*). *J Comp Physiol B* 181: 361–371, 2011. doi:10.1007/s00360-010-0532-4.
19. **Currie S, Edwards SL.** The curious case of the chemical composition of hagfish tissues–50 years on. *Comp Biochem Physiol A Mol Integr Physiol* 157: 111–115, 2010. doi:10.1016/j.cbpa.2010.06.164.
20. **Dvorak AM, Aird WC.** Endothelium in hagfish. In: *Hagfish Biology*, edited Edwards SL, Goss GG. Boca Raton, FL: CRC, 2015, p. 161–206. doi:10.1201/b18935-8.
21. **Edgar RC.** MUSCLE: multiple sequence alignment with high accuracy and high throughput. *Nucleic Acids Res* 32: 1792–1797, 2004. doi:10.1093/nar/gkh340.
22. **Edwards SL, Arnold J, Blair SD, Pray M, Bradley R, Erikson O, Walsh PJ.** Ammonia excretion in the Atlantic hagfish (*Myxine glutinosa*) and responses of an Rhc glycoprotein. *Am J Physiol Regul Integr Comp Physiol* 308: R769–R778, 2015. doi:10.1152/ajpregu.00355.2014.
23. **Evans DH.** Gill Na^+/H^+ and $Cl^-/^{HCO_3^-}$ exchange systems evolved before the vertebrates entered fresh water. *J Exp Biol* 113: 465–469, 1984.
24. **Frick NT, Wright PA.** Nitrogen metabolism and excretion in the mangrove killifish *Rivulus marmoratus* II. Significant ammonia volatilization in a teleost during air-exposure. *J Exp Biol* 205: 91–100, 2002.
25. **Galtier N, Gouy M, Gautier C.** SEAVIEW and PHYLO_WIN: two graphic tools for sequence alignment and molecular phylogeny. *Comput Appl Biosci* 12: 543–548, 1996.
26. **Glover CN, Bucking C, Wood CM.** Adaptations to *in situ* feeding: novel nutrient acquisition pathways in an ancient vertebrate. *Proc Biol Sci* 278: 3096–3101, 2011. doi:10.1098/rspb.2010.2784.
27. **Gouy M, Guindon S, Gascuel O.** SeaView version 4: A multiplatform graphical user interface for sequence alignment and phylogenetic tree building. *Mol Biol Evol* 27: 221–224, 2010. doi:10.1093/molbev/msp259.
28. **Hans M, Tabencka Z.** Über die Blutgefässe der Haut *Myxine glutinosa* L. *Bull Acad Pol Sci Ser BII Zool*: 69–77, 1938.
29. **Ip Y, Chew S, Leong I, Jin Y, Lim C, Wu R.** The sleeper *Bostrichthys sinensis* (family *Eleotridae*) stores glutamine and reduces ammonia production during aerial exposure. *J Comp Physiol B* 171: 357–367, 2001. doi:10.1007/s003600100184.
30. **Ip YK, Randall DJ, Kok TKT, Barzaghi C, Wright PA, Ballantyne JS, Wilson JM, Chew SF.** The giant mudskipper *Periophthalmodon schlosseri* facilitates active NH_4^+ excretion by increasing acid excretion and decreasing NH_3 permeability in the skin. *J Exp Biol* 207: 787–801, 2004. doi:10.1242/jeb.00788.
31. **Laemmli UK.** Cleavage of structural proteins during the assembly of the head of bacteriophage T4. *Nature* 227: 680–685, 1970. doi:10.1038/227680a0.
32. **Lametschwandtner A, Weiger T, Lametschwandtner U, Georgieva-Hanson V, Patzner RA, Adam H.** The vascularization of the skin of the Atlantic hagfish, *Myxine glutinosa* L. as revealed by scanning electron microscopy of the vascular corrosion casts. *Scanning Microsc* 3: 305–314, 1989.
33. **Le SQ, Gascuel O.** An improved general amino acid replacement matrix. *Mol Biol Evol* 25: 1307–1320, 2008. doi:10.1093/molbev/msn067.
34. **Malte H, Lomholt JP.** Ventilation and gas exchange. In: *The Biology of Hagfishes*, edited by Jørgensen JM, Lomholt JP, Weber RE, Malte H. Dordrecht, The Netherlands: Springer, 1998, p. 223–234. doi:10.1007/978-94-011-5834-3_14.
35. **Martini FH.** The ecology of hagfishes. In: *The Biology of Hagfishes*, edited by Jørgensen JM, Lomholt JP, Weber RE, Malte H. Dordrecht, The Netherlands: Springer, 1998, p. 57–77. doi:10.1007/978-94-011-5834-3_5.
36. **McDonald DG, Cavdek V, Calvert L, Milligan CL.** Acid-base regulation in the Atlantic hagfish *Myxine glutinosa*. *J Exp Biol* 161: 201–215, 1991.
37. **Miller MA, Pfeiffer W, Schwartz T.** Creating the CIPRES Science Gateway for inference of large phylogenetic trees. 2010 Gateway Comput Environments Workshop. New Orleans, LA, November 14, 2010. doi:10.1109/GCE.2010.5676129.
38. **Morris R.** Studies on salt and water balance in *Myxine glutinosa* (L.). *J Exp Biol* 42: 359–371, 1965.
39. **Potter IC, Welsch U, Wright GM, Honma Y, Chiba A.** Light and electron microscope studies of the dermal capillaries in three species of hagfishes and three species of lampreys. *J Zool (Lond)* 235: 677–688, 1995. doi:10.1111/j.1469-7998.1995.tb01777.x.
40. **Rauther M.** Kiemen der anamnier-kiemendarm-derivate der Cyclostomen und fische. Die driisenartigen derivate des kiemendarmes und kiemengange bei den Cyclostomen und fischen. In: *Handbuch der Vergleichenden Anatomie der Wirbeltiere*. Berlin: Urban & Schwarzenberg, 1937, p. 211–278.
41. **Sayer MD, Davenport J.** The relative importance of the gills to ammonia and urea excretion in five seawater and one freshwater teleost species. *J Fish Biol* 31: 561–570, 1987. doi:10.1111/j.1095-8649.1987.tb05258.x.
42. **Schultz AG, Guffey SC, Clifford AM, Goss GG.** Phosphate absorption across multiple epithelia in the Pacific hagfish (*Eptatretus stoutii*). *Am J Physiol Regul Integr Comp Physiol* 307: R643–R652, 2014. doi:10.1152/ajpregu.00443.2013.

43. **Smart G.** The effect of ammonia exposure on gill structure of the rainbow trout (*Salmo gairdneri*). *J Fish Biol* 8: 471–475, 1976. doi:10.1111/j.1095-8649.1976.tb03990.x.
44. **Smith CR, Baco AR.** Ecology of whale falls at the deep-sea floor. *Oceanogr Mar Biol* 41: 311–354, 2003.
45. **Stamatakis A.** RAxML version 8: a tool for phylogenetic analysis and post-analysis of large phylogenies. *Bioinformatics* 30: 1312–1313, 2014. doi:10.1093/bioinformatics/btu033.
46. **Strahan R.** The behaviour of myxinoids. *Acta Zoologica* 44: 73–102, 1963. doi:10.1111/j.1463-6395.1963.tb00402.x.
47. **Talavera G, Castresana J.** Improvement of phylogenies after removing divergent and ambiguously aligned blocks from protein sequence alignments. *Syst Biol* 56: 564–577, 2007. doi:10.1080/10635150701472164.
48. **Tsui TK, Randall DJ, Chew SF, Jin Y, Wilson JM, Ip YK.** Accumulation of ammonia in the body and NH(3) volatilization from alkaline regions of the body surface during ammonia loading and exposure to air in the weather loach *Misgurnus anguillicaudatus*. *J Exp Biol* 205: 651–659, 2002.
49. **Verdouw H, Van Echteld C, Dekkers E.** Ammonia determination based on indophenol formation with sodium salicylate. *Water Res* 12: 399–402, 1978. doi:10.1016/0043-1354(78)90107-0.
50. **Walsh PJ, Veauvy CM, McDonald MD, Pamenter ME, Buck LT, Wilkie MP.** Piscine insights into comparisons of anoxia tolerance, ammonia toxicity, stroke and hepatic encephalopathy. *Comp Biochem Physiol A Mol Integr Physiol* 147: 332–343, 2007. doi:10.1016/j.cbpa.2006.09.001.
51. **Weiner ID, Verlander JW.** Ammonia transport in the kidney by Rhesus glycoproteins. *Am J Physiol Renal Physiol* 306: F1107–F1120, 2014. doi:10.1152/ajprenal.00013.2014.
52. **Weinrauch AM, Edwards SL, Goss GG.** Anatomy of the Pacific hagfish (*Eptatretus stoutii*). In: *Hagfish Biology*, edited by Edwards SL, Goss GG. Boca Raton, FL: CRC, 2015, p. 1–40. doi:10.1201/b18935-2.
53. **Welsch U, Potter IC.** Dermal capillariesIn: *The Biology of Hagfishes*, edited by Jørgensen JM, Lomholt JP, Weber RE, Malte H. Dordrecht, The Netherlands: Springer, 1998, p. 273–283. doi:10.1007/978-94-011-5834-3_17.
54. **Wilkie MP, Clifford AM, Edwards SL, Goss GG.** Wide scope for nitrogen catabolism and urea excretion in the foraging Pacific hagfish. *Mar Biol* 164: 126, 2017. doi:10.1007/s00227-017-3148-3.
55. **Wilkie MP, Stecyk JAW, Couturier CS, Sidhu S, Sandvik GK, Nilsson GE.** Reversible brain swelling in crucian carp (*Carassius carassius*) and goldfish (*Carassius auratus*) in response to high external ammonia and anoxia. *Comp Biochem Physiol A Mol Integr Physiol* 184: 65–75, 2015. doi:10.1016/j.cbpa.2014.12.038.
56. **Wilson RW, Taylor EW.** Transbranchial ammonia gradients and acid-base responses to high external ammonia concentration in rainbow trout (*Oncorhynchus mykiss*) acclimated to different salinities. *J Exp Biol* 166: 95–112, 1992.
57. **Wright PA, Wood CM.** A new paradigm for ammonia excretion in aquatic animals: role of Rhesus (Rh) glycoproteins. *J Exp Biol* 212: 2303–2312, 2009. doi:10.1242/jeb.023085.
58. **Zimmer AM, Brauner CJ, Wood CM.** Ammonia transport across the skin of adult rainbow trout (*Oncorhynchus mykiss*) exposed to high environmental ammonia (HEA). *J Comp Physiol B* 184: 77–90, 2014. doi:10.1007/s00360-013-0784-x.